HHS Public Access

Author manuscript

Neuroimage. Author manuscript; available in PMC 2019 May 01.

Published in final edited form as:

Neuroimage. 2019 May 01; 191: 186–192. doi:10.1016/j.neuroimage.2019.02.017.

Prenatal lead exposure impacts cross-hemispheric and long-range connectivity in the human fetal brain

Moriah E. Thomason[*,1,2,3], **Jasmine L. Hect**[4], **Virginia A. Rauh**[5], **Christopher Trentacosta**[4], **Muriah D. Wheelock**[6], **Adam T. Eggebrecht**[7], **Claudia Espinoza-Heredia**[1], and **S. Alexandra Burt**[8]

[1]Department of Child and Adolescent Psychiatry, New York University Medical Center, New York, USA

[2]Department of Population Health, New York University Medical Center, New York, NY, USA

[3]Institute for Social Research, University of Michigan, Ann Arbor, MI, USA

[4]Department of Psychology, Wayne State University, Detroit, MI, USA

[5]The Heilbrunn Department of Population & Family Health, Columbia University Medical Center, New York, NY, USA

[6]Department of Psychiatry, Washington University in St. Louis, St. Louis, MO, USA

[7]Mallinckrodt Institute of Radiology, Washington University in St. Louis, St. Louis, MO, USA

[8]Department of Psychology, Michigan State University, East Lansing, MI, USA

Abstract

Lead represents a highly prevalent metal toxicant with potential to alter human biology in lasting ways. A population segment that is particularly vulnerable to the negative consequences of lead exposure is the human fetus, as exposure events occurring before birth are linked to varied and long-ranging negative health and behavioral outcomes. An area that has yet to be addressed is the potential that lead exposure during pregnancy alters brain development even before an individual is born. Here, we combine prenatal lead exposure information extracted from newborn bloodspots with the human fetal brain functional MRI data to assess whether neural network connectivity differs between lead-exposed and lead-naïve fetuses. We found that neural connectivity patterns differed in lead-exposed and comparison groups such that fetuses that were not exposed demonstrated stronger age-related increases in cross-hemispheric connectivity, while the lead-exposed group demonstrated stronger age-related increases in posterior cingulate cortex (PCC) to lateral prefrontal cortex (PFC) connectivity. These are the first results to demonstrate metal toxicant-related alterations in human fetal neural connectivity. Remarkably, the findings point to alterations in systems that support higher-order cognitive and regulatory functions. Objectives for

[*]**Corresponding Author:** Moriah E. Thomason, PhD, Department of Child and Adolescent Psychiatry, Department of Population Health, Child Study Center, One Park Avenue, 7th Floor, New York, NY 10016, T 646-754-5093, moriah.thomason@nyulangone.org.

future work are to replicate these results in larger samples and to test the possibility that these alterations may account for significant variation in future child cognitive and behavioral outcomes.

Keywords

brain; connectivity; fetal; lead; MRI; prenatal; resting-state

1. Introduction

Extensive epidemiological and clinical literature has documented the adverse effects of lead exposure in young children. In particular, exposure of the mother to heavy metal toxicants *during pregnancy* has been linked to offspring intellectual impairment (Canfield et al., 2004; Grandjean and Herz, 2015; Needleman et al., 1990), developmental disorders (Nuttall, 2017; Polanska et al., 2013), antisocial behavior (Dietrich et al., 2001; Wright et al., 2008), and adult neurological disorders (Mazumdar et al., 2012). Several accounts suggest that impairments in executive control and self-regulation may be core deficits cutting across these observed lead-associated phenotypes (Bellinger, 2011; Canfield et al., 2004; Schwartz et al., 2007; Schwartz et al., 2000). Despite consistent evidence of the harmful effects of prenatal lead exposure, mechanistic understanding of the processes by which exposure alters human development *in utero*, and how those alterations result in subsequent cognitive impairments and health risks is lacking. However, new developments in non-invasive fetal magnetic resonance imaging (MRI) avail unprecedented opportunity to directly evaluate the effects of prenatal lead, at the time that they occur, by performing *in vivo* measurements of fetal brain network development (Schopf et al., 2012; Thomason et al., 2013; van den Heuvel and Thomason, 2016). This advance makes it possible to evaluate how integrity of connections within and between separable fetal brain networks varies with presence of confirmed lead exposure during late stages of human pregnancy.

Observed effects of lead neurotoxicity on the central nervous system are widespread. Animal studies have demonstrated that early lead exposure is associated with reduced blood-brain-barrier integrity, altered myelination and synaptogenesis, increased iron deposition, and shifts in brain metabolic content (Zheng, 2001; Zhu et al., 2013). Results from magnetic resonance imaging studies in humans corroborate these effects, reporting altered myelin microstructure (Brubaker et al., 2009; Sahu et al., 2010), reduced structural brain volume (Brubaker et al., 2010; Cecil et al., 2008), altered brain metabolite levels (Cecil et al., 2011; Trope et al., 1998), and reduced activity in task-relevant brain circuitry (Yuan et al., 2006) in individuals exposed to lead. Furthermore, a subset of human imaging studies have linked MRI findings to individual differences in cognitive performance, suggesting brain changes are likely to be a key determinant in the neurobehavioral consequences of lead exposure (Schwartz et al., 2007). Despite this extensive cross-species documentation of the pervasive effects of lead on nervous system integrity and function, information about the effects of lead exposure on coordinated activity across large-scale brain systems is lacking. Additionally, while it is well-known that lead crosses the placenta and accumulates in fetal tissues (Gundacker and Hengstschlager, 2012), neurological studies of lead-exposure have yet to address the effects of lead-exposure measured directly in the *prenatal* human brain.

Recent advances in fetal resting-state functional connectivity (RSFC) MRI make it possible to perform non-invasive assessment of the connectional organization of human brain networks before birth (Schopf et al., 2012; Thomason et al., 2013; van den Heuvel and Thomason, 2016). RSFC MRI is a technique that relies on the assumption that areas that show coherence in patterns of functional activity over time during a resting, task-free state are anatomically and functionally connected to one another (Biswal et al., 1995; Smyser et al., 2011; Zhang and Raichle, 2010). This assumption is supported by demonstration that these covariance patterns map with high fidelity to anatomical architecture (Greicius et al., 2009; Honey et al., 2009). Application of the RSFC MRI approach to the fetal brain is relatively new (discussed in van den Heuvel and Thomason, 2016), but already this approach has led to new insights into normative processes of brain development (Schopf et al., 2012; Thomason et al., 2015), into alterations in neuroconnectivity that precede preterm birth (Thomason et al., 2017), and how variation in prenatal neuroconnectivity relates to infant motor outcomes (Thomason et al., 2018).

Here, we assess the hypothesis that intrauterine exposure to lead disrupts formation of human brain networks before birth. In a sample of typically-developing fetuses we evaluate associations between prenatal lead exposure and brain network integrity, measured using *in vivo* intrauterine fMRI. Based on newborn blood spot data we derived two subgroups, lead-exposed and lead naïve, that were matched in group size, and on demographic and health variables (Table 1). It is noteworthy that while we refer to the control cases as lead-naïve, some level of exposure may have been experienced in the control group at some point in pregnancy. Based on prior neurological and behavioral evidence that lead exposure may be particularly deleterious to prefrontal regions and executive control processes (Brubaker et al., 2010; Canfield et al., 2004; Cecil et al., 2008), we hypothesized brain regions important for cognitive and attentional control, for example areas that contribute to fronto-parietal and default-mode networks, and those in stages of rapid development in this time period, for example temporal and insular cortices, are most susceptible to effects of prenatal lead exposure.

2. Materials and Methods

2.1 Study design

Mothers were recruited during routine obstetrical appointments at Hutzel Women's Hospital in Detroit, Michigan during the second trimester of pregnancy. Inclusionary criteria included no contraindications for MRI, maternal age >18 years, and singleton pregnancy. 118 Mothers participated in 1 or 2 fetal brain MRI studies and completed questionnaires regarding thoughts, feelings, demographics, and health history. Medical birth records were obtained after delivery from two sources, with maternal consent: (1) Detroit Medical Center health records system, and (2) State of Michigan health records. Mothers provided written consent to access neonatal blood spots maintained by the Michigan Department of Health and Human Services (MDHHS) Newborn Screening Program.

2.2 Prenatal lead exposure assessment

For a subset of participants neonatal blood spot material was extracted from dried newborn bloodspot samples maintained by the MDHHS. Subject selection was based on a number of factors, including availability of samples and prior maternal consent, but also funding, as this was a pilot project. In brief, quality fetal fMRI data (all cases minimum 100 frames; average movement XYZ 0.233 mm and average PRY 0.165 deg) were available in 118 cases; of those, blood spot material were extracted for n = 72. A 6mm punch and card background material were extracted for each subject, and coded, deidentified samples were then transferred to the MDHHS Bureau of Laboratories (BOL), Division of Chemistry and Toxicology, Analytical Chemistry Section for analysis. MDHHS BOL is a College of American Pathologist (CAP) accredited laboratory. Each specimen was handled in the laboratory using universal precautions. The analysis was performed using a 3 mm punch that was removed from the original 6 mm punch, eluted and analyzed on a Perkin Elmer Nexion 300 ICP-MS following Division of Laboratory Sciences, National Center for Environmental Health laboratory procedure published standards (https://www.cdc.gov/nchs/data/nhanes/nhanes_09_10/pbcd_f_met.pdf). Lead content was analyzed and reported in units of micrograms of lead per deciliter of blood (μg/dL). The method reporting limit is 1.0 μg/dL and therefore values below 1.0 μg/dL were reported as < 1.0 μg/dL. Based on lead outcomes, equally-sized lead-exposed (N = 13; mean age at MRI = 33.69 +/− 4.28 weeks; 7 males) and lead-naïve (< 1.0 μg/dL; N = 13; mean age at MRI = 33.72 +/− 4.29 weeks; 6 males) comparison groups were defined for MRI analysis. Groups were matched on gestational age at scan (p = .80), gestational age at birth (p = .29), birth weight (p = .96), quantity of fMRI data analyzed after removing high-motion frames (U = .38), average translational motion (p = .59), average rotational motion (p = .66), and demographic variables, see Table 1. Groups also did not differ on maternal use of alcohol, drugs of abuse, or tobacco usage during pregnancy, with p-values ranging from .20 to .83.

2.3 MRI acquisition

Fetuses, age range 23.9 to 39.6 weeks gestational age, were scanned on a 3T Siemens Verio scanner equipped with a 4-channel abdominal flex coil. Functional images were collected using an echo planar image sequence sensitized to T2* weighted blood oxygenation level dependent (BOLD) signal changes. Dynamic fluctuation in BOLD signal intensity across brain regions, over time, corresponds with vascular response to oxygen delivery demands corresponding to concurrent brain activity. The result is a 4-dimensional record of activity across all brain areas over time. Specific parameters of the gradient echo sequence were as follows: 32 slices, repetition time TR = 2000 ms, echo time TE = 30, flip angle = 80°, resolution $3.4 \times 3.4 \times 4\ mm^3$. A total of 360 timeframes were collected in 12 minutes, and when possible, this sequence was repeated. MRI noise was minimized using earplugs and headphones (mother) and a custom-built belly band (fetuses) to minimize sound.

2.4 Fetal fMRI data preprocessing

Fetal RSFC data require extensive preprocessing prior to extraction of a whole brain connectional diagram, or connectome. We have developed a fetal-optimized MRI analysis pipeline that has been used in prior studies (Thomason et al., 2013; Thomason et al., 2015;

Thomason et al., 2017). The process begins with isolation of segments of >20 seconds of consecutive low-movement data. Timeframes falling within each low-motion segment are retained for further processing, and all other data are eliminated. Masks are generated for each segment, as fetal head position can change slightly between segments. The brain is manually traced in native image space to produce masks that are then applied using FSL (Smith et al., 2004). Following brain extraction, brains are reoriented into the standard imaging plane using SPM 8 (Statistical Parametric Mapping; http://www.fil.ion.ucl.ac.uk/spm/). Steps that follow are realignment and normalization into 2mm isotropic resolution fetal "template space" (Serag et al., 2012) to enable comparisons across subjects in the same coordinate space. Realignment and normalization are performed separately for each segment, then all data are concatenated, realigned (to correct misalignment between segments) and data are spatially smoothed at 4mm FWHM.

2.5 Whole-brain functional connectome construction

197 brain regions of interest (ROIs) were defined at the group level using spatially constrained spectral clustering (Craddock et al., 2012). In brief, this is a data-driven technique for defining approximately equally-sized, contiguous units (regions/nodes) that cover the full spatial extent of the cortex, subcortex and cerebellum. We then computed the strength of connectivity, or BOLD signal covariance, between every pair of regions using the Connectivity (CONN) FC Toolbox (ver.14n; www.nitrc.org/projects/ conn). Realignment parameters, with another six parameters representing their first order temporal derivatives, were removed with covariate regression analysis, and signals from white matter and cerebral spinal fluid were also regressed out using anatomical component correction (aCompCor; Behzadi et al., 2007; Chai et al., 2012). Band-pass filtering was set to $0.008 < f < 0.09$ Hz to remove the low frequency temporal drifts and high frequency physiological- and scanner-based artifact in the data. Functional connectivity values were then calculated as the pairwise zero-lag bivariate correlation between each of the 19,306 pairs of ROI timecourses, and then Fisher-z transformed. This resulted in a single 197 × 197 symmetrical adjacency matrix (a functional connectome) for each participant.

2.6 Statistical analyses

In order to test neural differences at the functional network level between lead-exposed and lead-naïve participant groups we implemented two parallel procedures. The first was to define subnetworks, following previously described routines (Eggebrecht et al., 2017), within the total brain architecture, based on data in the connectivity matrices described above. To achieve this objective fetal RSFC connectivity matrices from all available fetal cases, N = 118, were submitted to an Infomap community detection algorithm (Rosvall and Bergstrom, 2008) to generate a systems-wide functional network model composed of 16 unique subnetworks (Figure 1A). It was within these data-derived subnetworks that within- and between-network connectivity differences were subsequently tested. In parallel, to investigate the relationship between the RSFC data and gestational age (GA) for each group, we first calculated the Pearson correlation for each Fisher-z-transformed ROI-ROI RSFC pair against GA across subjects. Second, following previously developed methods (Eggebrecht et al., 2017; Marrus et al., 2018; McKinnon et al., 2018; Wheelock et al., 2018; Wheelock et al., (under review)), methods for enrichment analyses were adapted from those

used in largescale genomic association studies (Backes et al., 2014; Khatri et al., 2012; Rivals et al., 2007). For each study group, each within and between subnetwork pair was tested for enrichment of strong Pearson correlation values, defined as values remaining after being thresholded and binarized at an associated uncorrected P value ≤0.05. This process isolated all individual connections for which gestational age (GA) was significantly correlated with computed Fisher-z-transformed RSFC values.

Following these steps, we (1) used chi-square to test within-groups whether the number of significant edges within and/or between the derived subnetworks was significantly greater than chance, given the number of edges within/between each subnetwork, and (2) used the McNemar chi-square test to assess whether the pattern of significant edges within/between each subnetwork was significantly different between-groups. The chi-square test compares the observed number of strong RSFC-GA correlations within a functional network pair to the null hypothesis that assumes the overall number of strong correlations was uniformly distributed across all possible network pairs. The statistic is large when the number of strong correlations within a network pair is much less than (depletion) or much greater than (enrichment) expected. The McNemar statistic uses the number of discordant tests between study groups (b = number of ROI pairs True for lead-naive but false for lead-exposed, and c = the number of ROI pairs False for lead-naive but True at lead-exposed). For both the chi-square test of enrichment and the McNemar chi-square test across groups, data-driven empirical P values were calculated using randomization because permutation testing provides control over family-wise error rate, is nonparametric, automatically adjusts to the degree of correlation between tests, and does not make specific assumptions about the shape of the population distribution from which the observations have been derived (Backes et al., 2014). For each of 10,000 iterations, the subject pairing of RSFC and GA values was randomized to generate a false correlation statistic from which false within-group enrichment chi-square and across-group McNemar chi-square statistics were calculated to generate a null-distribution for each test. Within each iteration, asymptotic P values reflecting depletion were set to 1 to explicitly focus the statistical test on the probability of observing strong enrichment. The brain-wide permutation-based false-positive rate of the P values reflects the empirical probability of calculating the actual observed statistical value from all of the network blocks and represents a brain-wide null distribution for statistical evaluation of the data; thus, the P values presented below are empirically-derived permutation-based P values. This multi-tiered approach to within and between group connectome topography analysis has been employed and described in prior studies (Eggebrecht et al., 2017; Marrus et al., 2018; McKinnon et al., 2018; Wheelock et al., 2018; Wheelock et al., (under review)). The data and code used in this study will be made available via https://ndar.nih.gov/ and/or accessed upon direct request to M.E. Thomason (data) or A.T. Eggebrecht (code).

3. Results

3.1 Lead exposure groups

19.4% of N = 72 newborn bloodspots available for lead testing were positive for detectable levels of lead, ranging from 1 to 11 μg/dL with mean and standard error of the mean (SEM)

of 2.43(0.65) μg/dL. 19% is a high proportion of exposure, but this observation fits with prior reports indicating levels in Detroit are higher than national averages (Zhang et al., 2013). One subject with an estimated level of 7.4 μg/dL was removed from consideration due to a lack of usable fMRI data.

3.2 Age-related change in between- and within-network fetal brain connectivity

Lead-naïve and lead-exposed participant groups were separately assessed for changes in network properties with advancing gestational age. We observed age-related change in 7 network pairs in the lead-naïve group, compared to 4 in the lead-exposed group. For the lead-naïve group the most significant effect was seen in connectivity between the right temporal lobe and left posterior parietal cortex and the direction of this effect was predominately negative, denoting diminished connectivity between these regions at more advanced fetal age. For the lead-exposed group the most significant age-related effect was observed in connectivity within the right posterior parietal cortex and was predominately positive, denoting a strengthening of connectivity within parietal regions in older lead exposed fetuses. A complete summary of all between- and within-network pairs that showed significant age-related change in either study group is provided in Table 2.

3.3 Between-group differences in neural network connectivity

Lead-naïve participants exhibited age-related strengthening of cross-hemispheric connectivity that was not present in in the lead-exposed group. In particular, connectivity of bilateral insular cortices showed age-related effects in the lead-naïve group that was significantly greater than that observed in the lead-exposed group (Figure 2). The reverse was noted for connectivity between the superior frontal gyrus (SFG) and posterior cingulate cortex (PCC); lead-exposed fetuses demonstrated significantly greater age-related increases in connectivity between these networks than did lead-naïve fetuses.

4. Discussion

Growth processes occurring during human embryonic and fetal development are foundational to health and disease across the lifespan. Moreover, it is known that fetal exposure to environmental toxins such as lead can have profound influence on developmental outcomes. However, no prior research has examined the impact of lead exposure on developing fetal brain networks *in utero*. Here, we report differences in cross-hemispheric and anterior-posterior fetal brain connectivity that are associated with prenatal lead exposure. These results demonstrate that lead exposed fetuses deviate from typical patterns of brain development and suggest that altered neural connectivity may be a biological mechanism underlying poorer cognitive and behavioral outcomes in individuals exposed to lead during the prenatal period.

We observed significant age-related increase in cross-hemispheric connectivity in lead-naïve fetuses that was not observed in lead-exposed comparison subjects. Increased cross-hemispheric connectivity is a normative fetal brain maturational process (Jakab et al., 2014; Thomason et al., 2013) and absence of such early connectivity suggests delay toward attainment of neural connections that support intra-hemispheric information transfer.

Moreover, the areas involved in this lead-associated anomaly encompass areas of the insular, frontal and temporal cortices. These are particularly notable territories in the developing human brain, in part because they are the origin of spontaneous waves of activity that are postulated to support patterning of neural systems in the fetal brain (Arichi et al., 2017; Thomason, 2018). Results observed here are also align well with prior studies showing that childhood blood lead levels are associated with altered white matter microstructure (Brubaker et al., 2009; Sahu et al., 2010). Diminished connectivity *in utero* may precede long-term reduction in integrity of network structure, that in turn may contribute to cognitive deficits associated with neurotoxic insults from significant lead burden.

Another primary observation resulting from this novel comparison is that lead-exposed fetuses demonstrate augmented connectivity between lateral superior frontal gyrus (SFG) and the posterior cingulate cortex (PCC) with advancing age. This is of interest given that the SFG is a major constituent of the frontoparietal control network (FPN) whereas the PCC is a major constituent of the default mode network (DMN). This is a notable dichotomy given that activity in these networks is anticorrelated in the mature human brain, such that engagement of FPN is associated with diminished activity in the DMN and vice versa (Fox et al., 2005). The functional counterbalance between these systems is widely documented and has behavioral relevance. That is, engagement of the DMN is associated with introspective, stimulus-independent thought, and greater suppression of the DMN during attentionally-demanding tasks is associated with better performance (Hampson et al., 2010; Kelly et al., 2008; Thomason et al., 2008). Furthermore, both decrement in DMN suppression during task, and hyperconnectivity of the DMN, have been associated with psychopathology (Hamilton et al., 2011; Pomarol-Clotet et al., 2008; Whitfield-Gabrieli and Ford, 2012; Whitfield-Gabrieli et al., 2009). Overall, dynamic opposition between the FPN and DMN is regarded as a healthy feature of human brain functional network organization. Here we see the reverse in lead-exposed fetuses, *enhanced* positive FPC-DMN connectivity, a feature with potential to contribute to later developmental psychopathology and executive dysfunction.

It is noteworthy that neural effects associated with lead exposure are not ubiquitous across all brain areas, and instead show specificity. Here, we observe significant differences between two systems, and the direction of effects differs such that each group demonstrates augmented connectivity in one of the pairings. We interpret these as reflecting variation in the order and pattern with which brain subsystems and associated structures mature. This form of heterogeneity of observed neurological correlates of lead exposure has also been previously reported, for example, in the work of Brubaker and colleagues (2009) cited above. While this group observed widespread patterns of decreased fractional anisotropy in individuals with higher blood lead levels, they observed concomitant increase in radial MD in the corpus callosum and internal capsule, suggesting relatively higher myelin integrity (cf. Winklewski et al., 2018) in individuals with higher levels of lead exposure.

These data represent the first window into the immediate consequences of lead exposure in the human fetal brain, but these observations must be tempered by inherent limitations in our approach. The primary consideration is that the sample size (N = 26) may be underpowered to reliably detect significant effects. Having said this, the results surpassed significance

using data driven methodology, iterative permutation was used to set significance levels, and the results involve areas frequently implicated in lead-related neurotoxicity (Bellinger, 2011; Canfield et al., 2004; Cecil et al., 2008; Schwartz et al., 2007; Schwartz et al., 2000), suggesting that perhaps these are reliable early programming events that set the stage for future brain developmental processes. Nonetheless, pursuit of replication in a larger sample is warranted.

Another consideration is use of neonatal bloodspots for extracting lead exposure during late stages of pregnancy. Levels of detectable lead in a newborn bloodspot is an estimate covering approximately 28 days, coinciding with the half-life of lead. Reliance on this technique leaves us blind to what happened prior to 30 days before delivery, and moreover exposure is a dynamic process; a single snapshot cannot capture timing or exposure in aggregate. In addition, recent work has called into question the accuracy of lead estimates extracted from dried blood spots (Funk et al., 2015). A promising alternative for future work is to collect children's naturally shed deciduous teeth, as these contain biological signatures of metal exposures with temporal order beginning in week 15 of pregnancy (Modabbernia et al., 2016). An obvious drawback of this alternative is that collection of teeth can be impractical, but if possible, the upside would be an opportunity for evaluation of critical windows and mixture effects.

Two final considerations are that this small sample did not afford opportunity to examine sex-differences (cf. Cecil et al., 2008; Tong et al., 2000), or to link neural effects to variation in individual child outcomes. Both are significant future goals for the expanding exposome field of human developmental neuroscience. Indeed, it is well recognized that males and females demonstrate variation in sensitivity and vulnerability to insults in early development (Bale, 2016; Barnett and Scaramella, 2013; Góes et al., 2015; Whitfield et al., 1997). Further, it is essential to move beyond isolation of traits that differentiate exposure groups at a single timepoint, to follow development longitudinally to determine which of the observed effects precipitate developmental concerns, versus those that recover with developmental plasticity. These are utterly critical targets for future work that could offer core insight into predisposition for and consequences of neurological vulnerability to prenatal metal toxins.

In summary, two unprecedented observations have been achieved in this novel application of fetal fMRI to the formidable field of neurobiological consequences of lead exposure. Lead-exposed fetuses demonstrated relatively less age-related increase in cross-hemispheric connections and also exhibited heightened connectivity of the superior frontal gyrus and the posterior cingulate cortex with age. Both results suggest that the lead exposed group is deviating from typical patterns of development that involve both cross-hemispheric connectivity and negative signal coupling in lateral frontal control regions and the PCC.

Acknowledgements

The authors thank Janessa Manning, Sydney Townsel, Justin Bennett, Marjorie Beeghly, Jamie Percy, Jordan Boeve, Pavan Jella, Sophia Neuenfeldt, Toni Lewis, Tamara Qawasmeh for their assistance in data acquisition and analyses. We would also like to thank the participant families who generously shared their time. This work was supported by the National Institutes of Health [T32 MH100019 to MDW, K01 MH103594 to ATE, MH110793 and ES026022 to MET] and by a NARSAD Young Investigator Award to MET.

References

Arichi T, Whitehead K, Barone G, Pressler R, Padormo F, Edwards AD, Fabrizi L, 2017 Localization of spontaneous bursting neuronal activity in the preterm human brain with simultaneous EEG-fMRI. Elife 6.

Backes C, Ruhle F, Stoll M, Haas J, Frese K, Franke A, Lieb W, Wichmann HE, Weis T, Kloos W, Lenhof HP, Meese E, Katus H, Meder B, Keller A, 2014 Systematic permutation testing in GWAS pathway analyses: identification of genetic networks in dilated cardiomyopathy and ulcerative colitis. BMC Genomics 15, 622. [PubMed: 25052024]

Bale TL, 2016 The placenta and neurodevelopment: sex differences in prenatal vulnerability. Dialogues Clin Neurosci 18, 459–464. [PubMed: 28179817]

Barnett MA, Scaramella LV, 2013 Mothers' parenting and child sex differences in behavior problems among African American preschoolers. J Fam Psychol 27, 773–783. [PubMed: 23937420]

Behzadi Y, Restom K, Liau J, Liu TT, 2007 A component based noise correction method (CompCor) for BOLD and perfusion based fMRI. Neuroimage 37, 90–101. [PubMed: 17560126]

Bellinger D, 2011 The protean toxicities of lead: new chapters in a familiar story. Int J Environ Res Public Health 8, 2593–2628. [PubMed: 21845148]

Biswal B, Yetkin FZ, Haughton VM, Hyde JS, 1995 Functional connectivity in the motor cortex of resting human brain using echo-planar MRI. Magn Reson Med 34, 537–541. [PubMed: 8524021]

Brubaker CJ, Dietrich KN, Lanphear BP, Cecil KM, 2010 The influence of age of lead exposure on adult gray matter volume. Neurotoxicology 31, 259–266. [PubMed: 20226811]

Brubaker CJ, Schmithorst VJ, Haynes EN, Dietrich KN, Egelhoff JC, Lindquist DM, Lanphear BP, Cecil KM, 2009 Altered myelination and axonal integrity in adults with childhood lead exposure: a diffusion tensor imaging study. Neurotoxicology 30, 867–875.

Canfield RL, Gendle MH, Cory-Slechta DA, 2004 Impaired neuropsychological functioning in lead-exposed children. Dev Neuropsychol 26, 513–540. [PubMed: 15276907]

Cecil KM, Brubaker CJ, Adler CM, Dietrich KN, Altaye M, Egelhoff JC, Wessel S, Elangovan I, Hornung R, Jarvis K, Lanphear BP, 2008 Decreased brain volume in adults with childhood lead exposure. PLoS Med 5, e112. [PubMed: 18507499]

Cecil KM, Dietrich KN, Altaye M, Egelhoff JC, Lindquist DM, Brubaker CJ, Lanphear BP, 2011 Proton magnetic resonance spectroscopy in adults with childhood lead exposure. Environ Health Perspect 119, 403–408. [PubMed: 20947467]

Chai XJ, Castanon AN, Ongur D, Whitfield-Gabrieli S, 2012 Anticorrelations in resting state networks without global signal regression. Neuroimage 59, 1420–1428. [PubMed: 21889994]

Craddock RC, James GA, Holtzheimer PE, 3rd, Hu XP, Mayberg HS, 2012 A whole brain fMRI atlas generated via spatially constrained spectral clustering. Hum Brain Mapp 33, 1914–1928. [PubMed: 21769991]

Dietrich KN, Ris MD, Succop PA, Berger OG, Bornschein RL, 2001 Early exposure to lead and juvenile delinquency. Neurotoxicol Teratol 23, 511–518. [PubMed: 11792521]

Eggebrecht AT, Elison JT, Feczko E, Todorov A, Wolff JJ, Kandala S, Adams CM, Snyder AZ, Lewis JD, Estes AM, Zwaigenbaum L, Botteron KN, McKinstry RC, Constantino JN, Evans A, Hazlett HC, Dager S, Paterson SJ, Schultz RT, Styner MA, Gerig G, Das S, Kostopoulos P, Schlaggar BL, Petersen SE, Piven J, Pruett JR, Jr., 2017 Joint Attention and Brain Functional Connectivity in Infants and Toddlers. Cereb Cortex 27, 1709–1720. [PubMed: 28062515]

Fox MD, Snyder AZ, Vincent JL, Corbetta M, Van Essen DC, Raichle ME, 2005 The human brain is intrinsically organized into dynamic, anticorrelated functional networks. Proc Natl Acad Sci USA 102, 9673–9678. [PubMed: 15976020]

Funk W, Pleil J, Sauter D, McDade T, Holl J, 2015 Use of dried blood spots for estimating children's exposures to heavy metals in epidemiological research. Environmental & Analytical Toxicology S 7.

Góes F.V.d., Méio MDBB, Mello R.R.d., Morsch D, 2015 Evaluation of neurodevelopment of preterm infants using Bayley III scale. Revista Brasileira de Saúde Materno Infantil 15, 47–55.

Grandjean P, Herz KT, 2015 Trace elements as paradigms of developmental neurotoxicants: Lead, methylmercury and arsenic. J Trace Elem Med Biol 31, 130–134. [PubMed: 25175507]

Greicius MD, Supekar K, Menon V, Dougherty RF, 2009 Resting-state functional connectivity reflects structural connectivity in the default mode network. Cereb Cortex 19, 72–78. [PubMed: 18403396]

Gundacker C, Hengstschlager M, 2012 The role of the placenta in fetal exposure to heavy metals. Wien Med Wochenschr 162, 201–206. [PubMed: 22717874]

Hamilton JP, Furman DJ, Chang C, Thomason ME, Dennis E, Gotlib IH, 2011 Default-mode and task-positive network activity in major depressive disorder: implications for adaptive and maladaptive rumination. Biol Psychiatry 70, 327–333. [PubMed: 21459364]

Hampson M, Driesen N, Roth JK, Gore JC, Constable RT, 2010 Functional connectivity between task-positive and task-negative brain areas and its relation to working memory performance. Magn Reson Imaging 28, 1051–1057. [PubMed: 20409665]

Honey CJ, Sporns O, Cammoun L, Gigandet X, Thiran JP, Meuli R, Hagmann P, 2009 Predicting human resting-state functional connectivity from structural connectivity. Proceedings of the National Academy of Sciences of the United States of America 106, 2035–2040. [PubMed: 19188601]

Jakab A, Schwartz E, Kasprian G, Gruber GM, Prayer D, Schopf V, Langs G, 2014 Fetal functional imaging portrays heterogeneous development of emerging human brain networks. Front Hum Neurosci 8, 852. [PubMed: 25374531]

Kelly AM, Uddin LQ, Biswal BB, Castellanos FX, Milham MP, 2008 Competition between functional brain networks mediates behavioral variability. Neuroimage 39, 527–537. [PubMed: 17919929]

Khatri P, Sirota M, Butte AJ, 2012 Ten years of pathway analysis: current approaches and outstanding challenges. PLoS Comput Biol 8, e1002375. [PubMed: 22383865]

Marrus N, Eggebrecht AT, Todorov A, Elison JT, Wolff JJ, Cole L, Gao W, Pandey J, Shen MD, Swanson MR, Emerson RW, Klohr CL, Adams CM, Estes AM, Zwaigenbaum L, Botteron KN, McKinstry RC, Constantino JN, Evans AC, Hazlett HC, Dager SR, Paterson SJ, Schultz RT, Styner MA, Gerig G, Schlaggar BL, Piven J, Pruett JR, Jr., 2018 Walking, Gross Motor Development, and Brain Functional Connectivity in Infants and Toddlers. Cereb Cortex 28, 750–763. [PubMed: 29186388]

Mazumdar M, Xia W, Hofmann O, Gregas M, Ho Sui S, Hide W, Yang T, Needleman HL, Bellinger DC, 2012 Prenatal lead levels, plasma amyloid beta levels, and gene expression in young adulthood. Environ Health Perspect 120, 702–707. [PubMed: 22313790]

McKinnon CJ, Eggebrecht AT, Todorov A, Wolff JJ, Elison JT, Adams CM, Snyder AZ, Estes AM, Zwaigenbaum L, Botteron KN, McKinstry RC, Marrus N, Evans A, Hazlett HC, Dager SR, Paterson SJ, Pandey J, Schultz RT, Styner MA, Gerig G, Schlaggar BL, Petersen SE, Piven J, Pruett JR, Jr., 2018 Restricted and Repetitive Behavior and Brain Functional Connectivity in Infants at Risk for Developing Autism Spectrum Disorder. Biol Psychiatry Cogn Neurosci Neuroimaging.

Modabbernia A, Arora M, Reichenberg A, 2016 Environmental exposure to metals, neurodevelopment, and psychosis. Curr Opin Pediatr 28, 243–249. [PubMed: 26867166]

Needleman HL, Schell A, Bellinger D, Leviton A, Allred EN, 1990 The long-term effects of exposure to low doses of lead in childhood. An 11-year follow-up report. N Engl J Med 322, 83–88. [PubMed: 2294437]

Nuttall JR, 2017 The plausibility of maternal toxicant exposure and nutritional status as contributing factors to the risk of autism spectrum disorders. Nutr Neurosci 20, 209–218. [PubMed: 26613405]

Polanska K, Jurewicz J, Hanke W, 2013 Review of current evidence on the impact of pesticides, polychlorinated biphenyls and selected metals on attention deficit / hyperactivity disorder in children. Int J Occup Med Environ Health 26, 16–38. [PubMed: 23526196]

Pomarol-Clotet E, Salvador R, Sarro S, Gomar J, Vila F, Martinez A, Guerrero A, Ortiz-Gil J, Sans-Sansa B, Capdevila A, Cebamanos JM, McKenna PJ, 2008 Failure to deactivate in the prefrontal cortex in schizophrenia: dysfunction of the default mode network? Psychol Med 38, 1185–1193. [PubMed: 18507885]

Rivals I, Personnaz L, Taing L, Potier MC, 2007 Enrichment or depletion of a GO category within a class of genes: which test? Bioinformatics 23, 401–407. [PubMed: 17182697]

Rosvall M, Bergstrom C, 2008 Maps of random walks on complex networks reaveal community structure. PNAS 105, 1118–1123. [PubMed: 18216267]

Sahu JK, Sharma S, Kamate M, Kumar A, Gulati S, Kabra M, Kalra V, 2010 Lead encephalopathy in an infant mimicking a neurometabolic disorder. J Child Neurol 25, 390–392. [PubMed: 19633332]

Schopf V, Kasprian G, Brugger PC, Prayer D, 2012 Watching the fetal brain at 'rest'. Int J Dev Neurosci 30, 11–17. [PubMed: 22044604]

Schwartz BS, Chen S, Caffo B, Stewart WF, Bolla KI, Yousem D, Davatzikos C, 2007 Relations of brain volumes with cognitive function in males 45 years and older with past lead exposure. Neuroimage 37, 633–641. [PubMed: 17600728]

Schwartz BS, Stewart WF, Bolla KI, Simon PD, Bandeen-Roche K, Gordon PB, Links JM, Todd AC, 2000 Past adult lead exposure is associated with longitudinal decline in cognitive function. Neurology 55, 1144–1150. [PubMed: 11071492]

Serag A, Aljabar P, Ball G, Counsell SJ, Boardman JP, Rutherford MA, Edwards AD, Hajnal JV, Rueckert D, 2012 Construction of a consistent high-definition spatio-temporal atlas of the developing brain using adaptive kernel regression. Neuroimage 59, 2255–2265. [PubMed: 21985910]

Smith SM, Jenkinson M, Woolrich MW, Beckmann CF, Behrens TE, Johansen-Berg H, Bannister PR, De Luca M, Drobnjak I, Flitney DE, Niazy RK, Saunders J, Vickers J, Zhang Y, De Stefano N, Brady JM, Matthews PM, 2004 Advances in functional and structural MR image analysis and implementation as FSL. Neuroimage 23 Suppl 1, S208–219.

Smyser CD, Snyder AZ, Neil JJ, 2011 Functional connectivity MRI in infants: exploration of the functional organization of the developing brain. Neuroimage 56, 1437–1452. [PubMed: 21376813]

Thomason M, 2018 Structured Spontaneity: Building Circuits in the Human Prenatal Brain. Trends Neurosci 41, 1–3. [PubMed: 29224852]

Thomason M, Brown J, Dassanayake M, Shastri R, Marusak H, Hernandez-Andrade E, Yeo L, Mody S, Berman S, Hassan S, Romero R, 2014 Intrinsic functional brain architecture derived from graph theoretical analysis in the human fetus. Plos One.

Thomason M, Chang C, Glover G, Gabrieli J, Greicius M, Gotlib I, 2008 Default-mode function and task-induced deactivation have overlapping brain substrates in children. Neuroimage 41, 1493–1503. [PubMed: 18482851]

Thomason M, Dassanayake M, Shen S, Katkuri Y, Alexis M, Anderson A, Yeo L, Mody S, Hernandez-Andrade E, Hassan SS, Studholme C, Jeong JW, Romero R, 2013 Cross-hemispheric functional connectivity in the human fetal brain. Sci Transl Med 5.

Thomason ME, Grove LE, Lozon TA, Jr., Vila AM, Ye Y, Nye MJ, Manning JH, Pappas A, Hernandez-Andrade E, Yeo L, Mody S, Berman S, Hassan SS, Romero R, 2015 Age-related increases in long-range connectivity in fetal functional neural connectivity networks in utero. Dev Cogn Neurosci 11, 96–104. [PubMed: 25284273]

Thomason ME, Hect J, Waller R, Manning JH, Stacks AM, Beeghly M, Boeve JL, Wong K, van den Heuvel MI, Hernandez-Andrade E, Hassan SS, Romero R, 2018 Prenatal neural origins of infant motor development: Associations between fetal brain and infant motor development. Dev Psychopathol 30, 763–772. [PubMed: 30068433]

Thomason ME, Scheinost D, Manning JH, Grove LE, Hect J, Marshall N, Hernandez-Andrade E, Berman S, Pappas A, Yeo L, Hassan SS, Constable RT, Ment LR, Romero R, 2017 Weak functional connectivity in the human fetal brain prior to preterm birth. Sci Rep 7, 39286. [PubMed: 28067865]

Tong S, McMichael AJ, Baghurst PA, 2000 Interactions between environmental lead exposure and sociodemographic factors on cognitive development. Arch Environ Health 55, 330–335. [PubMed: 11063408]

Trope I, Lopez-Villegas D, Lenkinski RE, 1998 Magnetic resonance imaging and spectroscopy of regional brain structure in a 10-year-old boy with elevated blood lead levels. Pediatrics 101, E7.

van den Heuvel MI, Thomason ME, 2016 Functional Connectivity of the Human Brain in Utero. Trends Cogn Sci 20, 931–939. [PubMed: 27825537]

Wheelock MD, Austin NC, Bora S, Eggebrecht AT, Melzer TR, Woodward LJ, Smyser CD, 2018 Altered functional network connectivity relates to motor development in children born very preterm. Neuroimage 183, 574–583. [PubMed: 30144569]

Wheelock MD, Hect JL, Hernandez-Andrade E, Hassan SS, Romero R, Eggebrecht AT, Thomason ME, (under review). Sex differences in functional connectivity during fetal brain development Dev Cogn Neurosci.

Whitfield MF, Grunau RV, Holsti L, 1997 Extremely premature (< or = 800 g) schoolchildren: multiple areas of hidden disability. Arch Dis Child Fetal Neonatal Ed 77, F85–90. [PubMed: 9377151]

Whitfield-Gabrieli S, Ford JM, 2012 Default mode network activity and connectivity in psychopathology. Annu Rev Clin Psychol 8, 49–76. [PubMed: 22224834]

Whitfield-Gabrieli S, Thermenos HW, Milanovic S, Tsuang MT, Faraone SV, McCarley RW, Shenton ME, Green AI, Nieto-Castanon A, LaViolette P, Wojcik J, Gabrieli JD, Seidman LJ, 2009 Hyperactivity and hyperconnectivity of the default network in schizophrenia and in first-degree relatives of persons with schizophrenia. Proc Natl Acad Sci USA 106, 1279–1284. [PubMed: 19164577]

Winklewski PJ, Sabisz A, Naumczyk P, Jodzio K, Szurowska E, Szarmach A, 2018 Understanding the Physiopathology Behind Axial and Radial Diffusivity Changes-What Do We Know? Frontiers in neurology 9, 92–92. [PubMed: 29535676]

Wright JP, Dietrich KN, Ris MD, Hornung RW, Wessel SD, Lanphear BP, Ho M, Rae MN, 2008 Association of prenatal and childhood blood lead concentrations with criminal arrests in early adulthood. PLoS Med 5, e101. [PubMed: 18507497]

Yuan W, Holland SK, Cecil KM, Dietrich KN, Wessel SD, Altaye M, Hornung RW, Ris MD, Egelhoff JC, Lanphear BP, 2006 The impact of early childhood lead exposure on brain organization: a functional magnetic resonance imaging study of language function. Pediatrics 118, 971–977. [PubMed: 16950987]

Zhang D, Raichle ME, 2010 Disease and the brain's dark energy. Nat Rev Neurol 6, 15–28. [PubMed: 20057496]

Zhang N, Baker H, Tufts M, Raymond R, Salihu H, Elliott M, 2013 Early childhood lead exposure and academic achievement: evidence from Detroit public schools, 2008–2010. Am J Public Health 103, e72–77. [PubMed: 23327265]

Zheng W, 2001 Toxicology of choroid plexus: special reference to metal-induced neurotoxicities. Microsc Res Tech 52, 89–103. [PubMed: 11135452]

Zhu G, Fan G, Feng C, Li Y, Chen Y, Zhou F, Du G, Jiao H, Liu Z, Xiao X, Lin F, Yan J, 2013 The effect of lead exposure on brain iron homeostasis and the expression of DMT1/FP1 in the brain in developing and aged rats. Toxicol Lett 216, 108–123. [PubMed: 23219683]

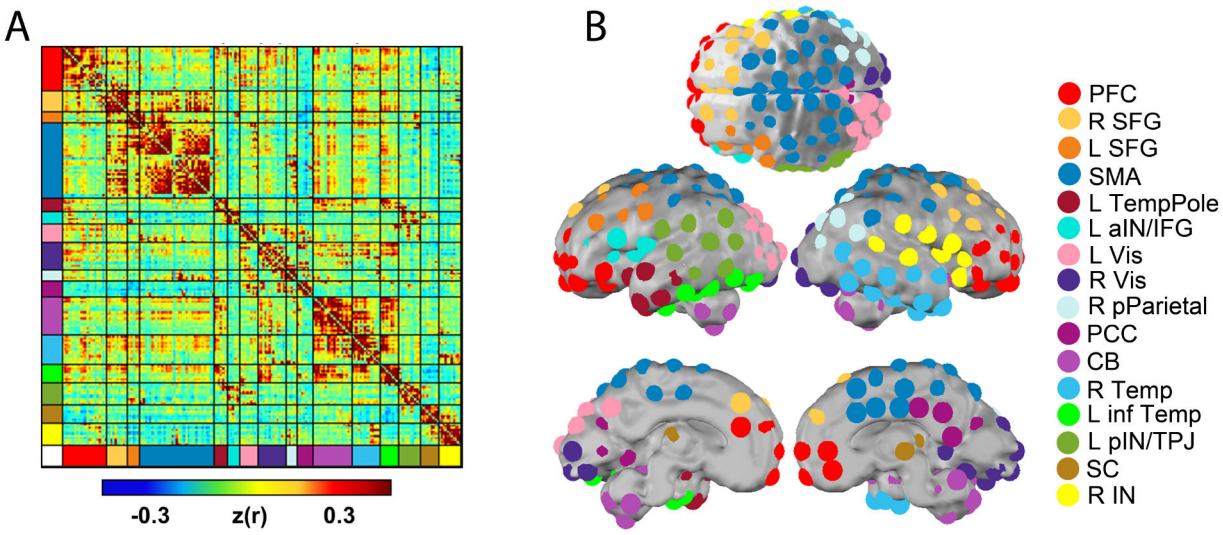

Figure 1. Fetal functional connectivity.

Panel A depicts an Infomap-sorted mean functional connectivity matrix derived from the correlation structure between 197 functionally defined ROIs. Panel B provides axial, lateral and midline views of the ROIs on the brain surface with coloring representing putative functional subnetworks.

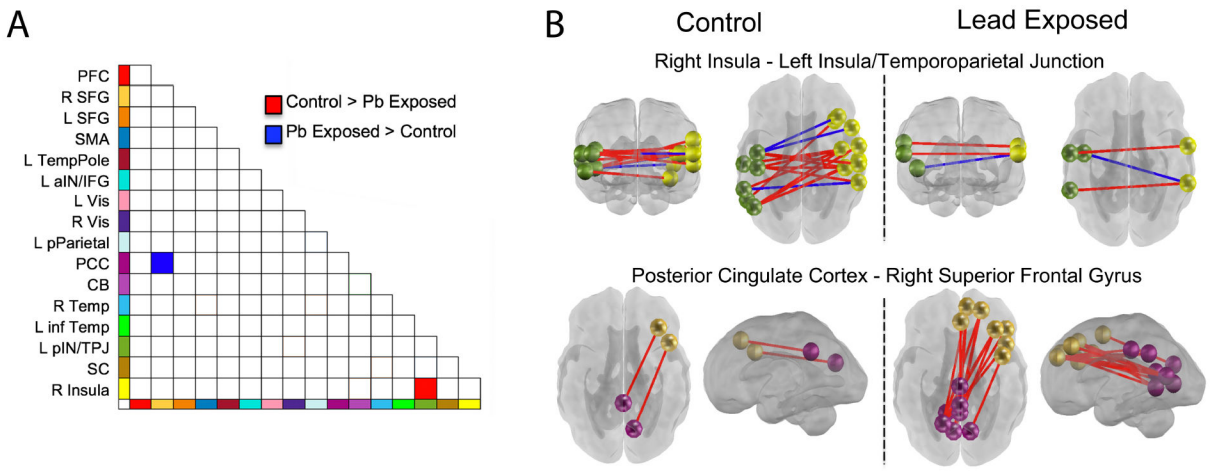

Figure 2. Lead-exposed and lead-naïve participant groups differences in neural connectivity between and across networks.

Differences were observed in two network pairs. Bi-lateral connectivity across insular-temporal cortices showed greater increase with age in lead-naïve fetuses (panel B upper), whereas lead-exposed fetuses showed a strengthening of lateral prefrontal (SFG) to posterior cingulate (PCC) connectivity with age that was not present in the comparison group (panel B lower). Both observations suggest lack of advancement of typical processes with the same rate in lead-exposed fetuses, as cross-hemispheric increases and reduced PCC-SFG have been observed as normative fetal brain developmental processes (Jakab et al., 2014; Thomason et al., 2014).

Table 1.

Summary of data and participant characteristics

	Lead Naïve (n=13)	Lead Exposed (n=13)	t / χ^2/ U	*p*
Birth Outcomes, *M (SD)*				
Fetal age at birth (weeks)	39.30 (1.61)	38.38 (1.78)	1.37	0.18
Birth weight (g)	3071 (633)	3067 (738)	0.02	0.99
Maternal Ethnicity, *n (%)*			1.53	0.68
African-American	9 (69.2)	11 (84.6)		
Asian-American	1 (7.7)	0		
Caucasian	2 (15.4)	1 (7.7)		
Bi-racial	1 (7.7)	1 (7.7)		
Maternal Education, *n (%)*			6.82	0.08
No GED/High-school diploma	0	2 (15.4)		
GED/High-school diploma	4 (30.8)	7 (53.8)		
Some college	9 (69.2)	3 (23.1)		
4-yr college degree	0	1 (7.7)		
Gross Annual Income, *n (%)*			6.72	0.15
< $10,000	3 (23.1)	9 (69.2)		
$10,000 - $20,000	2 (15.4)	72 (15.4)		
$20,000 - $30,000	3 (23.1)	1 (7.7)		
$50,000 - $60,000	2 (15.4)	0		
$60,000 - $80,000	0	1 (7.7)		
Undeclared	3 (23.1)	0		
Marital Status, *n (%)*			0.02	0.90
Single	8(61.5)	9 (69.2)		
Married/Partnered	4 (30.8)	4 (30.8)		
Undeclared	1 (7.7)	0		
Imaging Characteristics, *M (SD)*				
Maternal age at scan (years)	25.32 (4.98)	24.22 (4.56)	70.0	0.46
Fetal age at scan (weeks)	33.73 (4.29)	33.69 (4.28)	79.0	0.78
Amount of rs-fMRI data analyzed (minutes)	4.9 (1.8)	5.4 (1.9)	67.5	0.38
Translational mean movement (mm)	0.24 (0.13)	0.26 (0.11)	−0.55	0.59
Rotational mean movement (degrees)	0.45 (0.25)	0.49 (0.21)	−0.45	0.66

Two sample t-tests were used to assess differences between groups for age at birth, birth weight, translational motion, and rotational motion. Mann-Whitney U tests were used to examine differences for non-normally distributed, scalar variables (determined by Shapiro-Wilk Tests of Normality), including age at scan, frame count, and maternal age. Chi-square test was used to examine differences between groups for categorical variables, including ethnicity, education, income, and marital status. Due to small sample sizes, the Chi-square test assumption of each cell having a count of at least 5 was violated for all categorical variables. We observed that all comparisons provided above were non-significant, using two-tailed, $p < 0.05$.

Table 2.

Age-related network change in each group

	positive (%)	negative (%)	total N	Enrichment χ^2	Enrichment p-value	McNemar p-value
Lead exposed						
CB - CB	95	5	20	8.79	0.050	0.787
R pPar - R pPar	100	0	4	19.56	0.014	0.193
PCC - R SFG	100	0	15	21.53	0.011	0.023*
SC - L pIN/TPJ	43	57	14	10.65	0.038	0.405
Control						
	positive (%)	**negative (%)**	**total N**	**Enrichment χ^2**	**Enrichment p-value**	**McNemar p-value**
CB - CB	100	0	21	11.80	0.029	0.787
R Temp - SMA	21	79	48	9.58	0.040	0.083
R Temp - R pPar	0	100	10	8.42	0.048	0.154
L pIN/TPJ - R Vis	40	60	20	13.16	0.024	0.099
R Temp - SC	19	81	16	9.89	0.038	0.110
R IN - CB	96	4	24	10.97	0.032	0.079
R IN - L pIN/TPJ	80	20	15	8.66	0.046	0.031*

The number of significant connections within each network pair varies from region to region, and the proportion of those that are positive and negative also varies. Percentages denote proportion within each network pair that arose from significant positive or negative associations with age.

'Total N' denotes the number of total significant connections within each network pair. Enrichment χ^2 statistics and p-values describe the degree to which the number of significant ROI-ROI pairs within each network pair was greater than could be expected by chance. McNemar p-values describe the statistical difference between lead exposed and control fetal ROI-ROI connectivity within each network pair.